Effect of Glucose on the Distribution of Iodine-123-IHA-16 Between Esterification and Oxidation in Canine Myocardium

Charles C. Arvieux, Daniel Fagret, Francis Dubois, Pierre-Yves Brichon, Jean-Paul Mathieu, Paul Pilichowski, Pierre Cuchet, and Michel Comet

Laboratoire d'Etudes de Radiopharmaceutiques (URA CNRS 1287) and Laboratoire de Physiologie Animale (URA CNRS 632), Université Joseph Fourier, Grenoble, France

To evaluate the effect of glucose perfusion on the myocardial metabolism of [^{123}I]-16-iodo-9-hexadecenoic acid (IHA), the latter was injected intravenously into six fasting dogs perfused with a solution lacking glucose (controls) and seven fasting dogs perfused with glucose and insulin. The distribution of myocardial ^{123}I among iodides, free IHA, and esterified IHA was measured in myocardial biopsy specimens. The increase in esterification and decrease in oxidation of IHA due to glucose were quantified using a compartmental mathematical model of myocardial IHA metabolism. Subsequently, in six control and six glucose-perfused dogs, cardiac radioactivity was measured with a scintillation camera for 1 hr following i.v. injection of IHA. Four different methods were used to analyze the myocardial time-activity curves and to calculate the distribution of IHA between oxidation and esterification. Results comparable to those provided by analysis of biopsy specimens can be obtained by considering the curve to be the sum of an exponential and a constant, or by analyzing it with a compartmental mathematical model.

J Nucl Med 1990; 31:640–647

Free fatty acids (FFAs) and glucose are the two main energy sources of normally oxygenated myocardium. During fasting, FFAs are the major energy source: most of the internalized FFAs are degraded in the mitochondria, and the rest are esterified in the form of triglycerides and phospholipids. During feeding, blood glucose and insulin levels are relatively high, blood FFA levels are low, and glucose is the major fuel of the myocardium (*1*). Most of the internalized FFAs are esterified and stored in the cell, which is also the case during ischemia (*2*). The objective of the present study was to show that the in vivo distribution of myocardial FFAs between oxidation and esterification can be quantitated using [^{123}I]-16-iodo-9-hexadecenoic acid (IHA). The effect of glucose perfusion on the distribution of myocardial IHA between oxidation and esterification in the dog was first evaluated by studying myocardial biopsy specimens. Myocardial time-activity curves were then obtained with a scintillation camera after intravenous (i.v.) injection of IHA into dogs perfused with or without glucose, and were analyzed by different mathematical methods to determine which of them provided results comparable to the biopsy studies.

Received Mar. 28, 1989; revision accepted Dec. 21, 1989.

For reprints contact: Michel Comet, Laboratoire d'Etudes de Radiopharmaceutiques, Faculté de Médecine de Grenoble, 38700 La Tronche, France.

MATERIALS AND METHODS

Experimental Protocol

IHA (7 mg) was labeled with 148 MBq (4 mCi) of ^{123}I with a radiochemical yield higher than 90% as described elsewhere (*3*).

Experimental Preparation. After 24 hr fasting, dogs weighing between 15 and 25 kg were anesthetized by i.v. injection of thiopentone (induction dose 25 mg/kg^{-1}, maintenance dose 5 mg/kg^{-1} hr^{-1}). Intermittent ventilation (15 b.p.m.) with oxygen-enriched air at positive pressure was supplied via tracheal intubation. A peripheral vein was cannulated using a 16-gauge polyethylene cannula for continuous perfusion (10 ml kg^{-1} h^{-1}) of either an isotonic solution of NaCl (control dogs) or a 30% glucose solution containing 4 g of KCl and 60 IU l^{-1} insulin starting 1 hr before IHA injection and stopped 1 hr after IHA injection. The left common carotid artery was exposed in the neck and a stiff 14-gauge polyethylene cannula was inserted into the aorta for measurements of aortic blood pressure and withdrawal of blood samples for gas and biologic analyses. A similar catheter was inserted into the superior vena cava from the jugular vein to obtain blood samples for determining the time course of the IHA concentration.

Time Course of Plasma IHA. Blood samples (2 ml) were collected intravenously in a tube containing heparin 2, 4, 8, 15, 30, and 60 min after IHA injection, and the activity of each sample was measured. Proteins and red blood cells were denatured and lipophilic and hydrophilic products were separated after extraction in a mixture of isopropanol/heptane/1 N sulfuric acid (78:20:2, v/v). H_2O (2 ml) and heptane (4 ml) were then added and the mixture was vortexed for 1 min. The

two phases were separated by centrifugation at 850 g for 5 min. The volume of each phase was measured and 0.5-ml aliquots were counted for radioactivity. The aqueous phase was then percolated through Dowex anionic resin (AG 1×8, 200–400 mesh, Cl^- form) packed in acetone, which retained the iodides. The whole organic phase was concentrated under a hot nitrogen stream (~70°C) and applied to thin-layer chromatography (TLC) plates, which were developed in hexane/diethyl ether/acetic acid (80:50:0.5, v/v). IHA was thereby separated from iodine-labeled triglycerides and other chemical forms present at very low concentrations. The activity of the different fractions was measured with a Berthold 2B2842 scanner. To summarize, each sample was measured for total radioactivity and for the distribution of this activity among iodides, IHA, and triglycerides. Counts are expressed in cpm/ml^{-1}.

Myocardial Biopsies. Six control and seven glucose-perfused dogs were studied. After exposure by left thoracotomy, the heart was suspended in a pericardial cradle. Transmural biopsy specimens weighing 40–160 mg were then obtained with a rapidly spinning hollow needle (bore 4 mm) 0.5, 1.5, 5, 10, 30 and 60 min after IHA injection. Specimens were transferred to iced saline, washed, and squeezed in liquid nitrogen within 30 sec. Hemostasis was obtained with a narrow snare previously placed around the biopsy site. Biopsies were performed from the apical to the basal part of the left ventricular free wall in the regions of both the circumflex and the left anterior descending coronary arteries. Blood loss was <20 ml per biopsy, replaced with dextran solution. Biopsy specimens were ground in liquid nitrogen and lipids were extracted according to the method of Bligh and Dyer using ultrasound (*4*). Total radioactivity in each specimen and the radioactivity of its organic and aqueous phases were measured. The organic phase was analyzed by the procedure described above for plasma. An aliquot of the aqueous phase was applied to a reversed-phase TLC plate and developed in acetonitrile/H_2O/acetic acid (35:65:0.5, v/v) to assay for myocardial iodide. Since iodides can be found in plasma and in the interstitial and intracellular fluids, we subtracted the theoretical extracellular iodide activity from the iodide activity measured in each specimen. The theoretical value was determined by assuming that extracellular fluid represents 12% of myocardial tissue volume (*5*) and that the iodide concentration in interstitial fluid is the same as the plasma concentration at the same time. The results are expressed in cpm g^{-1} mCi injected.

Radionuclide Study. Six control and six glucose-perfused dogs were studied. A gamma camera equipped with a medium-energy collimator was placed over the thorax. A 20% window was used, centered around 159 keV. Thoracic radioactivity was measured for 60 min following IHA injection, and 1-min frames were obtained in a matrix of 64 × 64 pixels. The window was then centered at 140 keV and 370 MBq (10 mCi) of ^{99m}Tc-human serum albumin (Tc-HSA) was injected intravenously. Thoracic activity was recorded for 10 min postinjection.

Data Analysis

Myocardial Biopsies. Results were analyzed using a four-compartment mathematical model (*6*) (Fig. 1). Compartment V corresponds to intravascular IHA, Compartment 1 to intramyocardial free IHA, Compartment 2 to esterified forms of IHA and Compartment 3 to IHA degradation products. Compartment V exchanges IHA with all tissues, particularly with myocardium. The rate constants characterizing the model signify the following: k_{1v} corresponds to IHA uptake by myocardial cells, k_{v1} to back-diffusion, k_{21} to IHA esterification, k_{12} to lipolysis, k_{31} to mitochondrial degradation of IHA, and k_{03} to the release of degradation products into capillaries. The model is based on the following hypotheses:

1. IHA has zero or first-order kinetics.
2. The different rate constants do not change during measurement.
3. There is no intracellular synthesis of IHA from degradation products.
4. IHA degradation products released into capillaries cannot be taken up again.

The equations of the model are as follows:

$$q_v(t) = q_o[Ae^{-\alpha t} + (1 - A)e^{-\beta t}$$

$$q_1(t) = [k_{1v}q_v(t) + k_{12}q_2(t)]_* e^{-(k_{21}+k_{31}+k_{v1})t}$$

$$q_2(t) = k_{21}q_1(t)_* e^{-k_{12}t}$$

$$q_3(t) = k_{31}q_1(t)_* e^{-k_{03}t}$$

$$q_{mt}(t) = q_1(t) + q_2(t) + q_3(t),$$

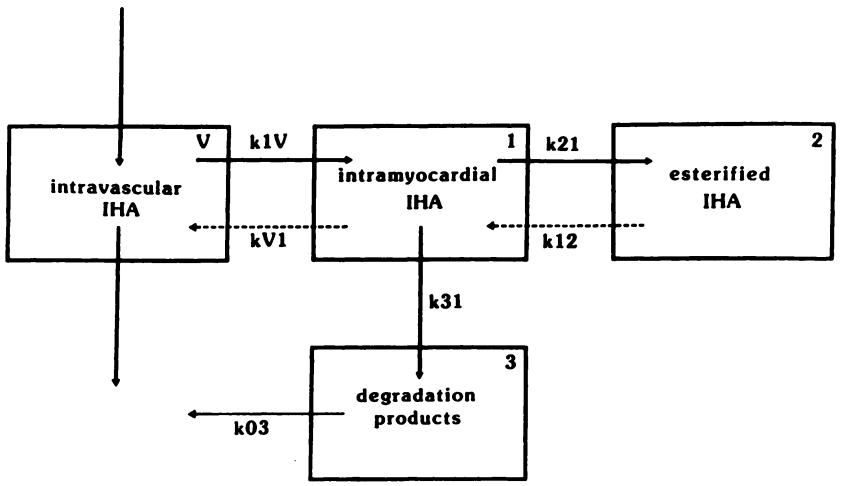

FIGURE 1
Compartmental mathematic model of the myocardial metabolism of iodinated fatty acids.

where $q_v(t)$, $q_1(t)$, $q_2(t)$, and $q_3(t)$ are the count rates, at time t, per gram and per mCi injected into compartments V, 1, 2, and 3, respectively; $q_{mt}(t)$ is the theoretical myocardial radioactivity per gram and per mCi injected; (*) is the convolution product. For each group of dogs, the count rates in the model compartments were fitted to the measured count rates as follows: $q_v(t)$ was obtained by calculating the mean of α, β and A determined in each dog by fitting the time courses of plasma IHA to the sum of a fast exponential with a half-life of

$$T_F = \frac{\ln 2}{\alpha}$$

and a slow exponential T_s

$$T_s = \frac{\ln 2}{\beta}.$$

$q_1(t)$ was fitted to the mean count rate of free IHA measured in the myocardium of each dog; the sum

$$[q_1(t) + q_2(t)]$$

was fitted to the mean count rate of the lipid phase, and lastly $q_3(t)$ was fitted to the mean count rate of the aqueous phase, which contained the iodinated degradation products of IHA. The three measured values were independent, i.e. an error in determining one of them did not affect the others. To obtain the values of:

$$k_{1v},\ (k_{21} + k_{31} + k_{v1}),\ k_{12},\ k_{03} \quad \text{and} \quad \frac{k_{21}}{k_{21} + k_{31}},$$

giving the best fit, we applied a Gauss-Newton algorithm, using the least squares method, to all three curves. The iterative process was stopped when the relative variation of the sum of the squares of the deviations between all measured values and the theoretical values of the model fell below 0.01.

To determine the dispersion of the rate constants, the calculation was repeated 25 times by randomly simulating the measured values of each point according to a gaussian law centered on the mean value, with the standard deviation (s.d.) equal to the standard error of the mean (s.e.m.) measured at each point (*7*). The mean value and the s.d. of the rate constants were determined in each of the 25 calculations. To determine which of the parameters of the model could be calculated precisely from the myocardial time-activity curve, we calculated the sensitivity function (*8*):

$$\frac{\delta q_{mt}(t)}{\delta p},$$

where $p = k_{12},\ k_{03},\ (k_{21} + k_{31} + k_{v1}),\ \frac{k_{21}}{k_{21} + k_{31}}$.

The mean sensitivity function was calculated for each value of p over all the measurement times, and the mean of the four sensitivity functions was then calculated. These values express the mean percentage of variation of the count rate per unit of p variation. The higher the sensitivity function of a rate constant, the more precisely it is determined, since a small change in its value leads to a large variation in the theoretical value of the count rate. When the sensitivity function of a rate constant is low, it cannot be determined precisely and only its order of magnitude can be obtained.

Radionuclide Study. To subtract background due to blood radioactivity (*9*) a region of interest (ROI) was drawn carefully around the heart (ROI1) and a second ROI over the large vessels at the base of the heart (ROI2) without encroaching upon the lungs or myocardium. Time-activity curves were plotted for each of the ROIs after injections of IHA and Tc-HSA. Following the IHA injection, the radioactivity q_c of ROI1 was equal to the sum of myocardial radioactivity q_m and blood radioactivity q_{b1}, i.e.:

$$q_c = q_m + q_{b1}.$$

The ratio of radioactivity q_{b2} in ROI2 to blood radioactivity q_{b1} in ROI1 remained at a constant K:

$$\frac{q_{b2}}{q_{b1}} = K.$$

Ten minutes after injection of Tc-HSA, K was obtained by calculating the ratio of ^{99m}Tc activity in ROI2 to that measured in ROI1. Knowing K, q_m could be calculated:

$$q_m = q_c - \frac{q_{b2}}{K}.$$

In this manner, image by image, blood activity was subtracted from total cardiac activity to obtain the time course of myocardial activity $q_m(t)$. To obtain an index of myocardial IHA uptake, the ratio of maximal myocardial activity per pixel to the radioactivity per pixel in ROI2 was measured 30 min after IHA injection.

Four methods for analyzing time-activity curves were used to evaluate the distribution of myocardial IHA between oxidation and esterification. All the theoretical curves were fitted to the myocardial time-activity curves with a Gauss-Newton algorithm using the least squares method.

Method 1: A single exponential was fitted to the descending part of the curve and its half-life was calculated.

Method 2: The descending part of the curve was considered to be the sum of a single exponential function and a constant activity (*10*) according to the equation:

$$Ae^{-\frac{\ln 2}{T}t} + B,$$

where B is a constant activity and T the half-life. This method assumes that the fraction

$$\frac{A}{A + B}$$

of intramyocardial IHA is oxidized and that the iodide is released from the myocardium with a half-life T. The fraction

$$\frac{B}{A + B}$$

of intramyocardial IHA is esterified.

Method 3: A, T, and B are adjusted to obtain the best fit of

$$q_v(t) * (Ae^{-\frac{\ln 2}{T}T} + B)$$

to the myocardial time-activity curve; $q_v(t)$ is the plasma IHA activity at time t and (*) is the convolution product. The fraction

$$\frac{B}{A + B}$$

is calculated as in Method 2.

Method 4: The compartmental mathematical model described above was used. The rate constant k_{12}, k_{03} and the ratio

$$\frac{k_{21}}{k_{21} + k_{31}}$$

were adjusted to obtain the best fit of $q_{mt}(t)$ to $q_m(t)$. The iteration process was stopped when the sum of the absolute values of the relative variation of

$$k_{12},\ k_{03} \quad \text{and} \quad \frac{k_{21}}{k_{21} + k_{31}}$$

was <0.05 between two iterations. The fit of theoretical curves to measured curves was evaluated by calculating the mean residual variation (MRV) defined by

$$MRV = \sqrt{\frac{\sum_i (Q_i - C_i)^2}{60}}.$$

The 60 measured values, O_i, and the 60 theoretical values, C_i, at time i are expressed as permillages of the maximum on the measured curve. The mean of the MRVs obtained with each of the four curve-analysis methods was calculated for the six control and six glucose-perfused dogs.

Reproducibility for Single Observers and Between Observers. To evaluate the effects of variable ROI determinations on the ratio:

$$\frac{k_{21}}{k_{21} + k_{31}},$$

10 studies were completely reprocessed 3 mo after the first determination, by two observers unaware of the first results. These results were subjected to analysis of variance.

Statistical Analysis. Differences between paired variables were assessed by paired t-tests ($p < 0.05$). Data are expressed as means ± s.d. Correlation between the results obtained by two calculation methods was assessed using the F ratio test.

RESULTS

Blood Analysis and Pressure-Rate Product (Table 1). The levels of blood glucose and FFA did not vary significantly during the hour in which the biopsies and scans were carried out in control dogs. Glucose perfusion caused a significant ($p < 0.05$) rise in blood glucose compared to the basal state. The FFA concentration, which varied considerably between dogs, did not decrease significantly during glucose perfusion. The product of systolic pressure and heart rate, calculated to evaluate the myocardial oxygen consumption and cardiac work, did not vary significantly during the biopsies and scans.

Plasma IHA Levels. Glucose perfusion led to a significant ($p < 0.05$) decrease in the IHA level until 8 min after IHA injection. Starting 15 min postinjection, IHA concentrations were <2% of the value measured 2 min postinjection and did not differ significantly between control and glucose-perfused dogs.

The mean half-life T_F of the fast exponential was significantly lower in the glucose-perfused dogs (1.099 ± 0.386 min^{-1} versus 1.499 ± 0.310 min^{-1}; $p < 0.02$). In contrast, the mean half-life, T_S, of the slow exponential decreased nonsignificantly during glucose perfusion (21.99 ± 11.03 min^{-1} versus 45.01 + 78.50 min^{-1}; ns). "A" did not differ significantly between glucose-perfused and control dogs (0.97 ± 0.01 versus 0.96 ± 0.02; ns).

Myocardial Biopsy. Glucose perfusion induced a significant ($p < 0.05$) increase in the percentage of FFA and esterified forms (triglycerides and phospholipids) and a significant ($p < 0.05$) decrease in the percentage of iodides with respect to total activity. In Figure 2, the theoretical curves obtained with the mathematical model are superimposed on the experimental values. Table 2 shows the rate constants calculated with the mathematical model. The rate constants

$$k_{12},\ k_{03} \quad \text{and} \quad \frac{k_{21}}{k_{21} + k_{31}}$$

were significantly ($p < 0.05$) higher during glucose perfusion.

TABLE 1
Mean Values (±s.d.) of the Pressure-Rate Products, Plasma Glucose and FFA Concentrations

		Biopsy			Scan		
		Glucose mM	FFA μM	P×HR mmHg b min^{-1}	Glucose mM	FFA μM	P×HR mmHg b min^{-1}
Control dogs	1	6.4 ± 1.4	282 ± 147	22,348 ± 3,686	6.6 ± 1.9	318 ± 110	24,842 ± 2,798
Control dogs	2	5.8 ± 1.7	322 ± 232	21,914 ± 3,849	6.2 ± 1.3	396 ± 331	28,161 ± 5,356
Glucose-Perfused dogs	0	5.9 ± 0.7	149 ± 179	—	7.1 ± 4.9	410 ± 324	—
	1	24.3* ± 16.2	—	24,904 ± 4,939	20.5* ± 14.13	—	26,329 ± 3,963
	2	17.8* ± 9.8	51 ± 52	24,092 ± 5,097	22.6* ± 19.8	93 ± 95	29,458 ± 7,714

*$p < 0.05$.

Mean values (±s.d.) of the pressure-rate products (P×HR) and the plasma glucose and FFA concentrations before glucose perfusion (O), before IHA injection (1) and 60 min after IHA injection (2). Six dogs were studied in each protocol.

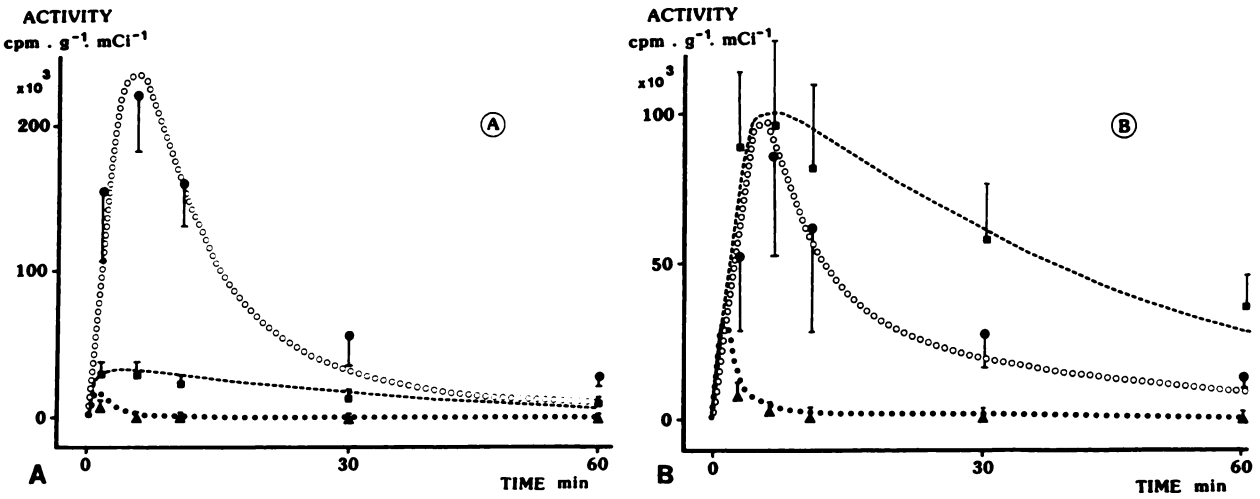

FIGURE 2

Means ± s.e.m. of radioactivity in iodides (○), free fatty acids (△), and esterified fatty acids (■) recovered from specimens of myocardial biopsies carried out 1.5, 5, 10, 30, and 60 min after IV injection of IHA, expressed as cpm g^{-1} mCi^{-1} injected. Theoretical curves of the time courses of radioactivity in iodides (○) free fatty acids (●), and esterified fatty acids (—), calculated with the mathematical model, are superimposed on the measured values. Panel A corresponds to control dogs and panel B to glucose-perfused dogs.

The first biopsy, carried out 30 sec after IHA injection, was too late to allow individual calculations of k_{v1}, k_{21}, and k_{31}. The value of the sum ($k_{21} + k_{31} + k_{v1}$) was estimated to be not <7 min^{-1} in control dogs, taking into account the IHA levels 30 sec postinjection.

Sensitivity Function. The sensitivity functions for the myocardial time-activity curve are given in Table 3. The highest values appeared with

$$k_{12},\ k_{03} \quad \text{and} \quad \frac{k_{21}}{k_{21} + k_{31}}.$$

The low values of the sensitivity function for the sum ($k_{v1} + k_{21} + k_{31}$) show that it cannot be calculated by analyzing the myocardial time-activity curve. The distribution of IHA between oxidation and esterification can most accurately be determined from the myocardial time-activity curve by calculating the ratio

$$\frac{k_{21}}{k_{21} + k_{31}}.$$

TABLE 2
Mean Values (±s.d.) of Rate Constants*

	Control dogs	Glucose-perfused dogs
k_{1v}	1.951 ± 0.361	1.715 ± 0.167
k_{12}	0.041 ± 0.010*	0.064 ± 0.0011
k_{03}	0.106 ± 0.035*	0.190 ± 0.032
$k_{21} + k_{31} + k_{v1}$	≥ 7	3.035 ± 0.511
$k_{21}/k_{21} + k_{31}$	0.141 ± 0.031*	0.424 ± 0.055

*$p < 0.05$

Constants are expressed per minute and calculated with the mathematical model from the activity measured in the biopsies.

Radionuclide Study. The mean myocardial IHA uptake index did not differ significantly between control and glucose-perfused dogs (1 ± 0.28 versus 0.84 ± 0.18; ns).

The values of the parameters given by the different methods used to analyze the myocardial time-activity curve are shown in Table 4. Glucose perfusion did not cause a significant variation of the mean half-lives given by Methods 1, 2, and 3. With Methods 2 and 3, the ratio

$$\frac{B}{A + B}$$

was significantly ($p < 0.05$) increased by glucose perfusion.

With Method 4, since the sensitivity function of the myocardial time-activity curve showed that only

$$k_{12},\ k_{03} \quad \text{and} \quad \frac{k_{21}}{k_{21} + k_{31}}$$

could be calculated (Table 4), the nonmeasurable sum ($k_{v1} + k_{21} + k_{31}$) was fixed at 3 min^{-1}. Glucose perfusion

TABLE 3
Sensitivity Functions of Myocardial Time-Activity Curves

p	Control dogs	Glucose-perfused dogs
k_{12}	595	331
k_{03}	159	711
$k_{v1} + k_{21} + k_{31}$	0.7	0.2
$k_{21}/k_{21} + k_{31}$	210	221

Myocardial time-activity curves are expressed as percentages of variation of the activity per gram of myocardium and per unit of p variation.

TABLE 4
Means (±s.d.) of Parameters Calculated by the Different Methods for Analyzing Myocardial Time-Activity Curves

	Method							
	1	2		3		4		
			$\frac{B}{A+B}$		$\frac{B}{A+B}$	$\frac{k_{21}}{k_{21}+k_{31}}$		
Method	T	T		T			k_{12}	k_{03}
Control dogs	26.3 ± 9	12 ± 3.8	0.15 ± 0.08	7.7 ± 0.6	0.10 ± 0.06	0.205 ± 0.123	0.018 ± 0.009	0.109 ± 0.017
Glucosed-Perfused dogs	53 ± 34	13.6 ± 3.9	0.35* ± 0.2	9.3 ± 2.9	0.22* ± 0.09	0.375* ± 0.109	0.016 ± 0.006	0.104 ± 0.044

*$p < 0.05$
The half-lives T are expressed in minutes and the rate constants are expressed per minute.

did not cause a significant variation of k_{12} or k_{03}, whereas the ratio

$$\frac{k_{21}}{k_{21} + k_{31}}$$

was significantly ($p < 0.05$) increased. Figure 3 shows the theoretical curve obtained with the mathematical model superimposed on the measured myocardial time-activity curve.

There was a close correlation between the ratios

$$\frac{B}{A + B}$$

given by Methods 2 and 3 ($r = 0.95$; $p < 0.01$). Moreover, the ratio

$$\frac{k_{21}}{k_{21} + k_{31}}$$

was closely correlated with the ratio

$$\frac{B}{A + B}$$

obtained by Methods 2 ($r = 0.87$; $p < 0.01$) and 3 ($r = 0.90$; $p < 0.01$), respectively. The MRV for the fit of an exponential function plus a constant to the descending part of the curve was lower than for the fit of an exponential function alone (28.1% ± 8.2% versus 56.7% ± 6.2%). Methods 3 and 4 take into account vascular IHA activity and can be fitted to the whole curve. The MRV for the fit with Method 4 was lower than that with Method 3 (48.8% ± 9.8% versus 56.7% ± 6.2%).

Reproducibility. Analysis of variance revealed no significant difference between the ratio

$$\frac{k_{21}}{k_{21} + k_{31}}$$

obtained by two observers or by the same observer 3 mo later ($F'39$ intraobserver: 0.73 NS; $F'39$ interobserver: 2.82 NS).

DISCUSSION

The distribution of myocardial fatty acids between oxidation and esterification depends on the nutritional state and the quality of myocardial oxygenation, among other conditions. After meals and during ischemia, fatty acids are mostly esterified in the form of triglycerides and phospholipids, whereas long after meals, well-oxygenated myocardium derives most of its energy from FFA oxidation (*1*). These variations of FFA distribution between oxidation and esterification, as well as the complementarity of glucose and FFA in supplying energy, have been demonstrated in myocardium using ^{11}C-palmitic acid and [^{18}F]fluorodeoxyglucose (*11,12*), whose use is limited. The objective of the present work in the dog was to show the possibility of using IHA to quantitate the distribution of myocardial FFA between oxidation and esterification. After its uptake by myocardial cells, IHA is partly degraded and partly esterified. The IHA molecule loses its iodine atom during mitochondrial β oxidation and there is no nonspecific

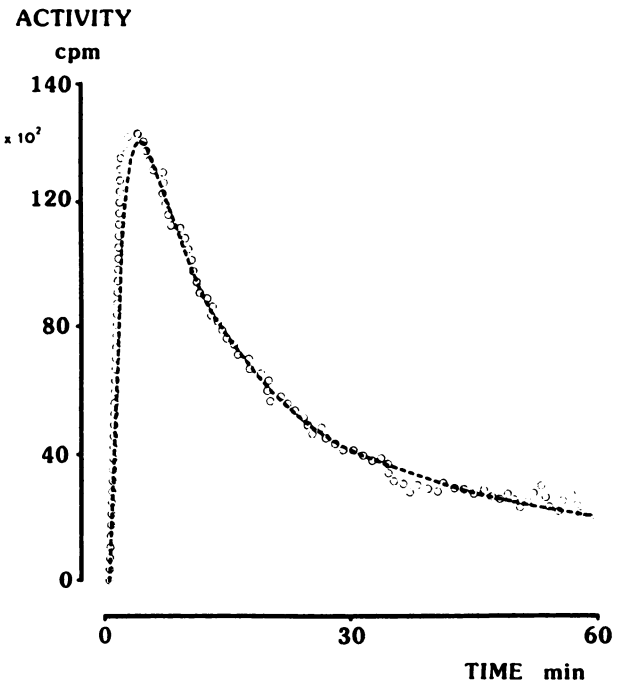

FIGURE 3
Theoretical curve obtained with the mathematical model (—) superimposed on the myocardial time-activity curve (O).

deiodination (*13*). Following i.v. injection of IHA in vivo, cardiac radioactivity can be measured by external detection and a time-activity curve can be plotted. It is then possible to determine the myocardial distribution of IHA between oxidation and esterification by analyzing the curve mathematically, on condition that a valid analytical method is used, i.e., that it has been shown to yield values in agreement with those measured experimentally in myocardial biopsy specimens.

For this reason, we first studied the effects of glucose perfusion on the distribution of myocardial IHA between oxidation and esterification by assaying specimens from myocardial biopsies carried out at fixed intervals following i.v. injection of IHA, according to a method proposed by Visser (*14*). Compared to control animals, glucose perfusion was found to increase the esterification of IHA in the form of triglycerides and phospholipids and to decrease its oxidation, as shown by the decrease in intracellular iodide. The shift in distribution between oxidation and esterification was quantified using a compartmental model of myocardial IHA metabolism, which has been validated in studies involving perfusion of isolated rat hearts (*6*). The model takes into account the time course of plasma IHA, which is fitted with the sum of a fast exponential and a slow exponential. The half-life of the fast exponential is comparable to that measured in the dog using ^{14}C-palmitic acid (*15*). In glucose-perfused dogs, the half-lives of the fast exponential were significantly shorter than those in control animals. These results are comparable to those obtained in studies of plasmatic ^{14}C-palmitate clearance in humans after ingestion of glucose (*16*). Glucose perfusion produced a small but significant rise in k_{12} and k_{03}, representing lipolysis and iodide release from cells, respectively. The increase in esterification and decrease in oxidation due to glucose were expressed by a significant rise in the ratio

$$\frac{k_{21}}{k_{21} + k_{31}}.$$

The individual values of k_{21} and k_{31}, expressing esterification and oxidation respectively, could not be calculated because the phenomena were too rapid, particularly in the absence of glucose. Nor was it possible to calculate k_{v1}, which expresses back-diffusion. During normal oxygenation, back-diffusion is of the order of 15% of the FFA taken up, whereas during ischemia it reaches 44% (*17,18*).

In a second series of experiments in control and glucose-perfused dogs, IHA was injected intravenously and the cardiac time-activity curve was determined with a scintillation camera for 60 min (*9*). Cardiac radioactivity is here the sum of myocardial and circulatory radioactivity. The latter arises from IHA, iodinated triglycerides, and especially radioactive iodide from IHA oxidation. The fraction of circulatory radioactivity in the total cardiac count, estimated to amount to ~75% (*19*), is not constant since it depends on the volume of the cardiac cavities. If it is not subtracted, only results of the same patient can be compared and not those of different patients (*20*). Several methods have been proposed for subtracting it, but none of them escape criticism (*19*). Comparison of results obtained with different subtraction techniques must take into account the fact that the cardiac time-activity curve depends: (a) on the input function represented by the time course of plasma IHA (*12*), (b) on myocardial IHA metabolism, and (c) on circulatory activity. A method involving Tc-HSA was used in the present study and has been shown to yield reproducible results in the dog (*21*).

Glucose perfusion led to a nonsignificant decrease in the myocardial IHA uptake index, whereas studies carried out with ^{11}C-palmitate have shown a large decrease in the uptake (*12*). Several methods for analyzing myocardial time-activity curves were compared with regard to their accuracy in evaluating the distribution of intramyocardial IHA between oxidation and esterification. The first, proposed by Poe (*22*), consisted in fitting the descending portion of the curve with an exponential, whose half-life was calculated. The increase in esterification was expressed by a nonsignificant increase in the half-life. This did not give a good fit with the experimental curve, as shown by the high MRV (*10*). The second method involved fitting the descending part of the curve with the sum of an exponential and a constant B (*10*):

$$Ae^{-\frac{\ln 2}{T}t} + B.$$

The half-life T of the exponential quantifies myocardial iodide release and the ratio

$$\frac{B}{A + B}$$

quantifies the fraction of intramyocardial IHA that is esterified. Glucose perfusion led to a statistically significant increase in

$$\frac{B}{A + B}$$

whereas the half-life T did not vary. Similar results have been obtained in humans (*20*). The sum of an exponential and a constant provided a better fit with the descending part of the curve than a simple exponential, and showed the distribution between oxidation and esterification of the IHA taken up.

Two other methods (3 and 4) took into account the time course of plasma IHA (input function) and could be used to analyze the whole curve. Method 3 consisted in finding the sum of an exponential and a constant, which, when convoluted with time course of plasma IHA, yielded a good fit with the myocardial time-

activity curve. As with Method 2, the ratio

$$\frac{B}{A + B}$$

thereby calculated was significantly higher in the glucose-perfused dogs, whereas the half-lives of the exponential did not differ between the two groups of animals. Method 4 consisted in analyzing the curve with a compartmental model of myocardial IHA metabolism (*6*). The individual values of the constants k_{21} and k_{31}, representing esterification and oxidation respectively, could not be calculated since the processes were too fast and only the ratio

$$\frac{k_{21}}{k^{21} + k^{31}}$$

could be calculated.

Glucose perfusion significantly increased this ratio. The theoretical curve given by the model provided a better fit with the experimental curve than that obtained with Method 3, and the variability of ROI determination by a single observer or between two observers had no effect on the results of the ratio. There was a good correlation between the values of distribution between oxidation and esterification obtained with Methods 2, 3, and 4.

In conclusion, the variation in distribution between oxidation and esterification induced in the dog by glucose perfusion can be evaluated by analyzing the myocardial time-activity curves with the three methods proposed. More experience is needed before a definitive choice can be made between them. The measurements were performed under normal oxygen conditions, during which back-diffusion is negligible. Using ^{11}C-palmitate, Schelbert et al. (*23*) have shown that during certain cardiomyopathies, myocardium responds abnormally to glucose input by increasing fatty acid oxidation. Consequently, measurement of IHA distribution between oxidation and esterification following glucose perfusion could be clinically useful during nonischemic cardiomyopathies. During ischemia, back-diffusion is no longer negligible, and the validity of measuring IHA distribution between oxidation and esterification remains to be demonstrated in this case.

ACKNOWLEDGMENT

This work was supported by grants from the Scientific Council of the "Faculté de Médecine de Grenoble" and from the "Fondation pour la Recherche Médicale."

REFERENCES

1. Opie LH. Metabolic response during impending myocardial infarction. I. Relevance of studies of glucose and fatty acid metabolism in animals. *Circulation* 1972; 45:483–490.
2. Scheuer J, Brachfeld N. Myocardial uptake and fractional distribution of palmitate-1-^{14}C by the ischemic dog heart. *Metabolism* 1966; 15:945–954.
3. Riche F, Mathieu JP, Comet M, et al. Synthesis of 16-iodo-9-hexadecenoic acid labelled with iodine-123. *Radiochem Radioanal Lett* 1982; 53:225–230.
4. Bligh RG, Dyer WJ. A rapid method of total lipid extraction and purification. *Can J Biochem Physiol* 1959;37:911–917.
5. Gerdes AM, Kasten FH. Morphometric study of endomyocardium and epimyocardium of the left ventricle in adult dogs. *Am J Anat* 1980; 159:389–394.
6. Dubois F, Depresseux JC, Bontemps L, et al. Mathematical model of the metabolism of ^{123}I-16-iodo-9-hexadecenoic acid in an isolated rat heart. Validation by comparison with experimental measurements. *Eur J Nucl Med* 1986; 11:453–458.
7. Graham MM. Model simplification: complexity versus reduction. *Circulation* 1985;72 (suppl I):63–67.
8. Tomovic R. *Sensitivity analysis of dynamic systems.* New York: McGraw Hill; 1964.
9. Comet M. Experimental studies on myocardial metabolism of iodinated fatty acids: a proposal for a new curve analysis technique. In: Van Der Wall EE, ed. *Noninvasive imaging of myocardial metabolism.* New York: Martinus Nijhoff Publishers; 1987; 109–125.
10. Van Eenige MJ, Visser FC, Duwel CMB, et al. Analysis of myocardial time-activity curves of ^{123}I-heptadecanoic acid. I. Curve fitting. *Nucl Med* 1987; 26:241–247.
11. Schelbert HR. Probing the heart's biochemistry with positron emission tomography. *Jap Circ J* 1986; 50:1–29.
12. Schelbert HR, Henze E, Schon HR, et al. C-11 palmitate for the noninvasive evaluation of regional myocardial fatty acid metabolism with positron computed tomography. III. In vivo demonstration of the effects of substrate availability on myocardial metabolism. *Am Heart J* 1983; 105:492–504.
13. Cuchet P, Demaison L, Bontemps L, et al. Do iodinated fatty acids undergo a nonspecific deiodination in the myocardium? *Eur J Nucl Med* 1985; 10:505–510.
14. Visser FC, Van Eenige MJ, Westera G, et al. Metabolic fate of radioiodinated heptadecanoic acid in the normal canine heart. *Circulation* 1985; 72:565–571.
15. Bierman EL, Schwartz IL, Dole VP. Action of insulin on release of fatty acids from tissue stores. *Am J Physiol* 1957; 191:359–362.
16. Waterhouse C, Kemperman JH. Changes in oxidative metabolism with glucose ingestion. *J Lab Clin Med* 1966; 68:250–264.
17. Fox KAA, Abendschein DR, Ambos HD, et al. Efflux of metabolized and nonmetabolized fatty acid from canine myocardium. *Circ Res* 1985; 57:232–243.
18. Rosamond TL, Abendschein DR, Sobel BE, Bergmann SR, Fox KAA. Metabolic fate of radiolabeled palmitate in ischemic canine myocardium: Implications for positron emission tomography. *J Nucl Med* 1987; 28:1322–1329.
19. Van Eenige MJ, Visser FC, Van Lingen A, Van Der Wall EE, Heidendal GAK, Roos JP. Evaluation of background correction methods. *Eur Heart J* 1985; 6(suppl B):57–59.
20. Duwel CMB, Visser FC, Van Eenige MJ, Van Der Lugt HAM, Roos JP. The influence of glucose on the myocardial time-activity curve during 17-iodo-123 heptadecanoic acid scintigraphy. Nucl Med Commun. 1987; 8:207–215.
21. Comet M, Wolf JE, Pilichowski P, et al. Scintigraphie myocardique après injection I.V. d'acide ^{123}I-hexadécène-9-oïque. Etude de la reproductibilité des résultats chez le chien. *J Biophys et Med Nucl* 1983; 7:139–145.
22. Poe ND, Robinson GD, Graham LS, MacDonald NS. Experimental imaging with ^{123}I-labeled hexadecenoic acid. *J Nucl Med* 1976; 17:1077–1082.
23. Schelbert HR, Henze E, Sochor H, et al. Effects of substrate availability on myocardial C-11 palmitate kinetics by positron emission tomography in normal subjects and patients with ventricular dysfunction. *Am Heart J* 1986; 111:1055–1064.